water

Article

Application of Machine Learning Techniques for the Estimation of the Safety Factor in Slope Stability Analysis

Yaser Ahangari Nanehkaran [1], Tolga Pusatli [2], Jin Chengyong [3], Junde Chen [4], Ahmed Cemiloglu [1], Mohammad Azarafza [5] and Reza Derakhshani [6,*]

[1] School of Information Engineering, Yancheng Teachers University, Yancheng 224002, China
[2] Department of Management Information Systems, Cankaya University, Ankara 06790, Turkey
[3] Academy of Engineering & Technology, Yang-En University, Quanzhou 362014, China
[4] Department of Electronic Commerce, Xiangtan University, Xiangtan 411100, China
[5] Department of Civil Engineering, University of Tabriz, Tabriz 5166616471, Iran
[6] Department of Earth Sciences, Utrecht University, 3584 CB Utrecht, The Netherlands
* Correspondence: r.derakhshani@uu.nl

Abstract: Slope stability is the most important stage in the stabilization process for different scale slopes, and it is dictated by the factor of safety (FS). The FS is a relationship between the geotechnical characteristics and the slope behavior under various loading conditions. Thus, the application of an accurate procedure to estimate the FS can lead to a fast and precise decision during the stabilization process. In this regard, using computational models that can be operated accurately is strongly needed. The performance of five different machine learning models to predict the slope safety factors was investigated in this study, which included multilayer perceptron (MLP), support vector machines (SVM), k-nearest neighbors (k-NN), decision tree (DT), and random forest (RF). The main objective of this article is to evaluate and optimize the various machine learning-based predictive models regarding FS calculations, which play a key role in conducting appropriate stabilization methods and stabilizing the slopes. As input to the predictive models, geo-engineering index parameters, such as slope height (H), total slope angle (β), dry density (γ_d), cohesion (c), and internal friction angle (φ), which were estimated for 70 slopes in the South Pars region (southwest of Iran), were considered to predict the FS properly. To prepare the training and testing data sets from the main database, the primary set was randomly divided and applied to all predictive models. The predicted FS results were obtained for testing (30% of the primary data set) and training (70% of the primary data set) for all MLP, SVM, k-NN, DT, and RF models. The models were verified by using a confusion matrix and errors table to conclude the accuracy evaluation indexes (i.e., accuracy, precision, recall, and f1-score), mean squared error (MSE), mean absolute error (MAE), and root mean square error (RMSE). According to the results of this study, the MLP model had the highest evaluation with a precision of 0.938 and an accuracy of 0.90. In addition, the estimated error rate for the MLP model was MAE = 0.103367, MSE = 0.102566, and RMSE = 0.098470.

Keywords: slope stability; factor of safety; machine learning; prediction; soil slope

check for updates

Citation: Ahangari Nanehkaran, Y.; Pusatli, T.; Chengyong, J.; Chen, J.; Cemiloglu, A.; Azarafza, M.; Derakhshani, R. Application of Machine Learning Techniques for the Estimation of the Safety Factor in Slope Stability Analysis. *Water* **2022**, *14*, 3743. https://doi.org/10.3390/w14223743

Academic Editors: Zhaoli Wang, Yaolong Zhao and Weilin Liao

Received: 28 September 2022
Accepted: 13 November 2022
Published: 18 November 2022

1. Introduction

Slope stability is one of the most important topics of geotechnical engineering, with a background of more than 300 years. Simple evaluations, planar failure, limit state criteria, limit equilibrium analysis, numerical methods, hybrid and high-order approaches, and implementation in both two and three dimensions are just some of the stability assessment techniques that have been developed [1,2]. The purpose of a slope stability analysis is to assess the stability of slopes (both excavated and natural) experiencing sliding movements [3]. The slope stability is considered the most extensive description for soil and rock (or a combination of both) slope masses under various failures [4], which is essentially controlled by the ratio between the available shear strength and the acting shear stress, which can be expressed in terms of a factor of safety (FS) if these quantities are integrated over a potential sliding surface [5,6]. Under certain conditions, these failures can cause damage, which is directly dependent on the geological conditions of the slope mass [7].

Generally, the type of slope failure directly depends on the geological units and constituent geomaterials, geometric characteristics, stress–strain background, geostructural and tectonic conditions, geomorphology status, regional climate, seismic activity, water conditions (surface and underground), vegetation, weathering, drainage pattern, construction activities, and the special condition of the slope [8,9]. The stability of a slope is calculated by the FS, which represents the general or local stability status of the slope. The FS is computed along any potential sliding surface running from the top of the slope to its toe. An FS equal to 1 is considered a critical state. The smallest FS value will be taken as representing the instability condition of the slope [3]. Limit equilibrium analysis methods (LEMs), one of the fundamental and traditional analytical approaches for slope stability analyses, can be used to calculate FS and are frequently used in slope stability studies due to the fact of their simplicity, low formulation complexity, and short computational times [10]. The static and dynamic conditions for two- and three-dimensional space [5,6] are both possible to use with LEMs based on massive or slice analysis. LEMs investigate a possible slippery mass at the top of the assumed slip surface and the polyhedral force vector closure or incurring moments in an equilibrium state. If all assumptions and requirements are met and the polyhedral forces are closed, then the mass must be in equilibrium. When the polyhedral forces and moments do not add up to zero (the force vectors are not closed), this means there are not enough of the right values for some of the effective parameters to calculate [11]. The various equilibrium methods are utilized to estimate the FS. Some of the more well-known of these methods can be stated as OMS/Fellenius, Bishop, Janbu, modified Swedish, Lowe–Karafiath, Morgenstern–Price, and USACE methods [7]. Most of these methods provide close results in calculating the factor of safety (FS), and the difference in the estimated values is usually less than 6% [12]. The majority of the limit equilibrium approaches use the Mohr–Coulomb relation to estimate the shear stress and resistance across the slip surface in all types of failures, where this criterion is considered one of the most important failure criteria for stability analyses in geomaterials [13]. Based on LEMs, the FS coefficient is defined for different slip surface force equilibrium methods, and the moment equilibrium method is based on a limit equilibrium, where the shear stress/resistance is considered as the total resistance–stress or effective resistance–stress. In the force equilibrium method, the ratio of the resisting forces to the mobilized forces at the possible slip surface is investigated, and in the moment method, by comparing the resistant moments to the overturning moments, the reliability of the slope is estimated. According to their achievements, these methods are capable of being applied to various types of slope failures or complex movements [14].

The evaluation uncertainties in FS values make it difficult for traditional stability analysis methods to provide accurate results, which are affected by the stabilization process. To cover this problem, scholars used computational intelligence approaches. In the meantime, machine learning techniques have received excellent attention for reducing uncertainties in FS calculations. Zhou et al. [15] used the gradient boosting machine (GBM) technique to estimate the FS and its relationship with triggering factors on slope instabilities. Wei et al. [16] used support vector regression (SVR) and radius basis function (RBF) to predict the FS based on geotechnical parameters. The findings suggest that RBF is superior to other methods for FS prediction. Qi et al. [17] used various artificial intelligence-based classifiers to predict the FS values with proper accuracy for slopes, which was applied for slope stabilization. Bai et al. [18] provide comparative machine learning-based predictive models to predict the FS for slopes, which were appropriately implemented for stability analysis. The present study attempted to use various machine learning-based predictive models to provide more accurate predictions for the FS based on the relative influencing factors. Zhang et al. [19] introduced a GPR-based predictive model for slope stability evaluations, which was useful to apply as a comparative assessment with common machine learning methods, such as

MLP and SVM. Chakraborty and Goswami [20] used the MLP model to estimate the FS, and the model was validated via numerical finite element codes. Jagan et al. [21] used various types of learning classifiers, such as ANFIS, GPR, RVM, and ELM, for layered slope stability assessments. Bui et al. [22] showed that machine learning-based models can be considered a reliable alternative for FS estimations for different types of slopes and failures. Bardhan and Samui [23] used MLP and marine predator algorithm (MPA) models to predict the FS for the high soil slope of the heavy-haul railway embankment in India. The model was verified by the GeoStudio program. Karir et al. [24] used various machine learning models to predict and obtain the FS values for both natural and man-made slopes. Omar et al. [25] used MLP- and ANFIS-based predictive models as well as LEMs to analyze the stability of a layered slope. The predictive models provided good agreement results for FS evaluations.

The present study attempted to use a comparative analysis of several machine learning methods, including multilayer perceptron (MLP), support vector machines (SVM), k-nearest neighbors (k-NN), decision tree (DT), and random forest (RF), to predict the FS values for different slopes by using geotechnical properties. The main goal of the study was to provide a highly accurate predicting procedure by using these predictive models. In this regard, a suitable database from the south Pars region in Iran was provided and used to train and test the algorithms. Various statistical indices such as error tables were employed to calculate the error and correlation between the real and predicted FS data.

2. Materials and Methods

2.1. Geotechnical Database

In order to provide the primary database, a comprehensive field survey was conducted in the South Pars region, located in southwest Iran. A total of 70 slopes were identified for a stability analysis along with geotechnical investigations. The geomechanical properties were estimated for a slope by taking samples of the soils and performing geotechnical index laboratory tests, such as unconfined compression [26] and direct-shear [27] tests, same as conducted for the field topological recordings. The instructions for the field studies, sampling, and testing were provided by American Society for Testing and Materials (ASTM) organizations, and they are comprehensively described in geotechnical books. To estimate the engineering properties, samples were taken, isolated (to prevent changes in a sample's water content), transported to the laboratory, prepared, and tested. These geo-engineering index parameters can be categorized as slope height (H), total slope angle (β), dry density (γ_d), cohesion (c), and internal friction angle (φ). These five features that were used to prepare the primary database reflect the basic geometrical and mechanical aspects of the slope condition. The samples were taken in summer in dry conditions, and the ratio of the pore water pressure was not applied in the assessments. It should be noted that the pore water pressure is one of the most important factors in stability assessments and has to be considered in the FS calculations. Although this factor was not included in the present study due to the lack of pore water pressure, machine learning models can consider this factor as an input parameter if it is available and use it during prediction processes. In general, changes in the input parameters can affect the final results of predictive models, but it does not have much impact on the forecasting process. Nevertheless, the pore water pressure ratio (if it is applicable) has to be considered in evaluations.

The prepared database was used for the training and testing of entire machine learning classifiers. Table 1 provides information regarding the geotechnical features that were measured from the laboratory and field investigations.

Table 1. Geotechnical characteristics of the studied slopes.

Parameter	Unit	Maximum	Minimum	Mean	SD
Water content	%	6.22	1.73	3.97	2.24
Specific gravity (G_s)	-	2.85	2.49	2.67	0.16
γ_d	kN/m^3	18.99	18.69	18.84	0.18
Slope height	m	135	12	73.5	50.21
Slope angle	Degree	77	43	60	13.88
Cohesion (c)	kPa	97	39	68	23.9
Friction (φ)	Degree	35	20	27.5	7.51

2.2. Data Acquisition

Following the preparation of the primary database, the database was labeled and its features were categorized. In this regard, the estimated values of an FS less than 1.00 were categorized as unstable, 1.00 to 1.50 as attention-required, and greater than 1.50 as stable. As is known, this classification is an empirically recommended system by professionals that can be applied to different cases [28–31]. In fact, due to the uncertainty and complexity of the slope, it was difficult to analyze the slope stability in general form, so it had to be analyzed for each slope and to obtain the FS_{min}, which represents the probable sliding surface by LEMs. This classification was used in the predictive models to describe the slope conditions. The FS was estimated based on the relationship between the slope stability factor (which represents the slope durability condition) and the geo-engineering characteristics, which were established through the training process by different machine learning classifiers. Regarding the slope stability analysis methods, the FS can be calculated based on the polyhedral force vector closure or incurring moments in an equilibrium state at an assumed slip surface for two-dimensional and three-dimensional spaces, which is responsible for static failure, with the moveable mass weight and geometry as the geotechnical characteristics (Table 1) of the slope, as defined in this equation.

$$\mathrm{FS} = \frac{\sum \text{Resistance forces or moments}}{\sum \text{Activation forces or moments}} = f(\gamma_d, H, c, \phi, \beta)$$

Before the training process starts, the gathered data have to be normalized. Figure 1 illustrates the standardized data variation for the primary database by using a box plot. A box plot is a statistical representation of the distribution of a variable through its quartiles. The ends of the box represent the lower and upper levels of the variations, and the body indicates the concentration of the data. Based on this figure, it can be stated that the distribution of the φ and β values are approximately similar, the distribution of H is wider, and the distribution of the c and γ_d values is more concentrated for slopes.

As mentioned, the FS is responsible for failure in the slope and is estimated by using the geo-engineering characteristics of the slope, which represent the slope behavior. The pair-wise relationships between all recorded slope data are shown in Figure 2. Regarding this figure, the relationship between the index parameters that are used as inputs in machine learning predictive models was investigated. The result shows that the geometrical features, such as H and β, are relative, as are c and γ_d. Using this correlation can help in estimating the certain overlap between the geo-engineering characteristics and the FS specified. The off-diagonal plots that are presented in Figure 2 are related to stable and unstable slopes and indicate that the stable and unstable zones were concentrated in different regions. Thus, each feature has to be considered as having an independent role in evaluating the slope stability.

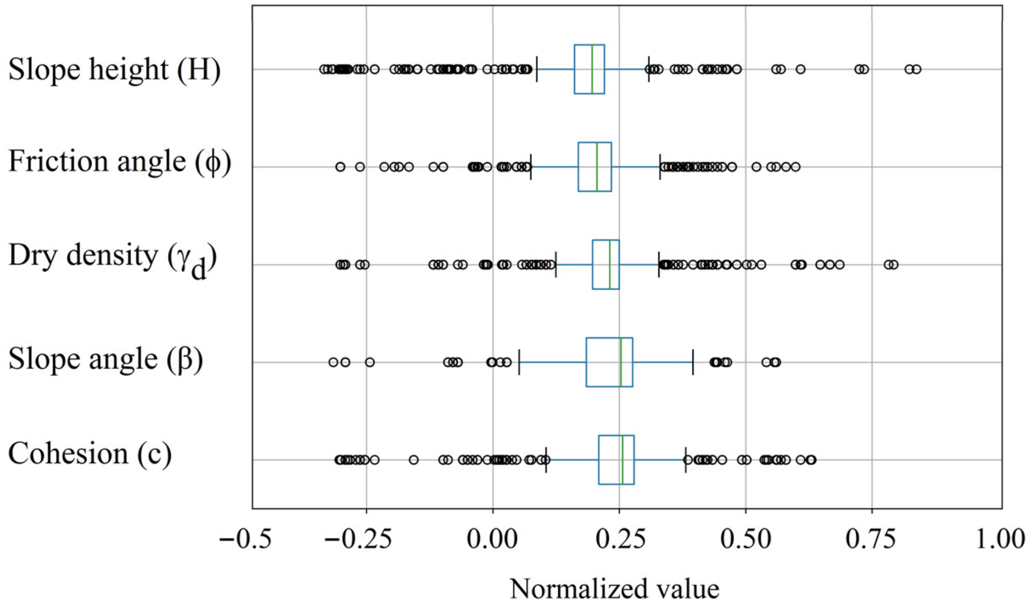

Figure 1. Results of the box diagram for the standardized data.

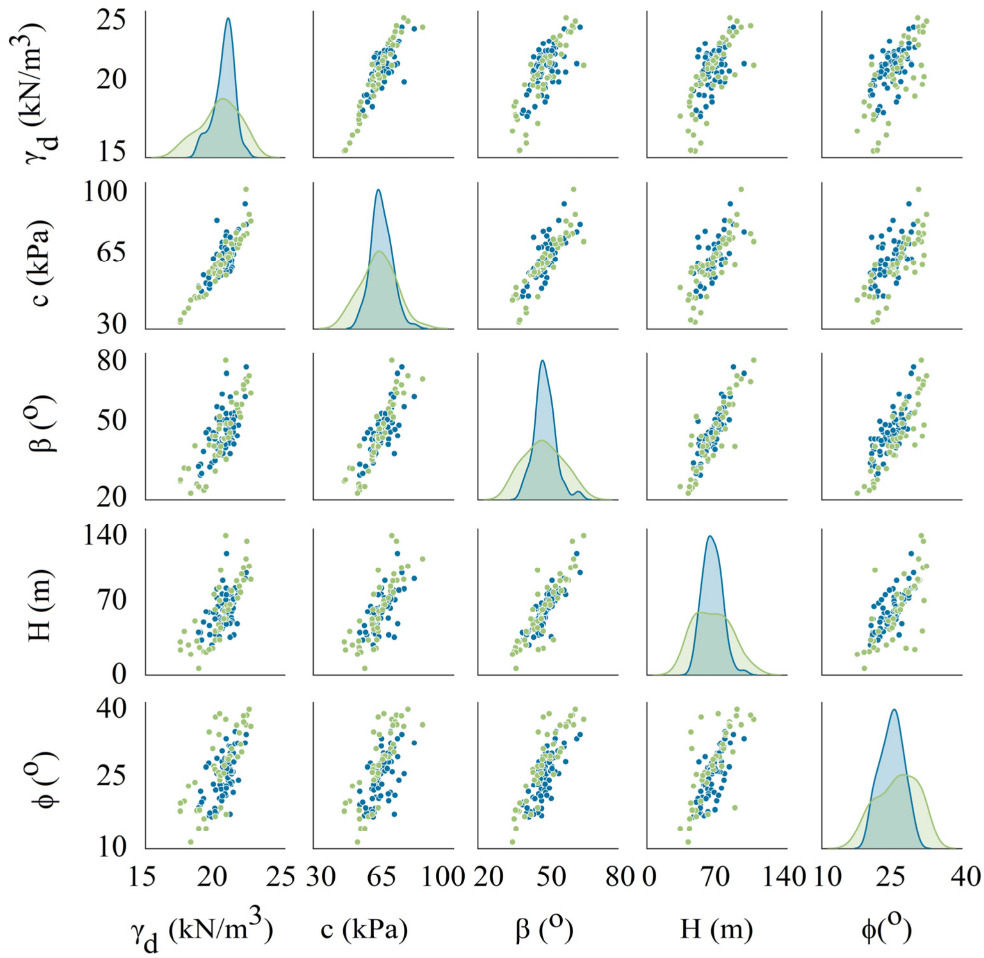

Figure 2. Results of the correlation analysis of the index parameters (green: stable; blue: unstable).

2.3. Predictive Model Implementations and Adjustment

The prepared database was divided into training and testing sets at random. The training set covered 70% of the primary database, while the testing set covered 30%. Both stability and instability cells were used to fit the predictive models. The algorithms were written in Python, a high-level programming language. The models used the TensorFlow and Keras libraries for implementations. These libraries are known as Python interfaces for artificial neural networks and classifiers. A training set is a subset of a larger data set that is used to fit (train) a model for predicting values that are known in the training set but unknown in the testing data. The training set is used in conjunction with the validation and/or test sets to evaluate various models. By the training set, we mean that the model will be trained on the training data set using a supervised learning method, such as gradient descent or stochastic gradient descent. In practice, the training data set is frequently made up of pairs of an input vector (or scalar) and the corresponding output vector (or scalar), with the answer key commonly referred to as the target (or label). The target in the present study is FS values. A testing set, on the other hand, is a secondary (or tertiary) data set used to put a machine learning program to the test after it has been trained on an initial training data set. The test data set is a set of data used to provide an unbiased assessment of the final model fit on the training data set. The model learning rate, or the response to the estimated error each time the model weights are updated, depends on the test/train ratio. In actuality, the model's learning rate determines how quickly it adapts to the problem. Smaller learning rates result in slower changes to the weights at each update and need more training epochs, whereas larger learning rates produce faster changes and need fewer training epochs. In particular, the learning rate is a hyperparameter that can be customized and used to train neural networks. Its value is typically small and positive, falling between 0.0 and 1.0. The learning rate used in this study was chosen by optimizers, which were scheduled via callbacks in Keras support for 0.01 and no momentum. Table 2 provides the hyperparameter for the ideal values of the machine learning-based models used in this article.

Table 2. The hyperparameters used by applied predictive models.

Classifier	Hyperparameters	Elements
Multilayer perceptron (MLP)	Hidden layers' size Learning rate Optimization	Activation = 'relu'; Optimization = 'rmsprop'; Loss_function = 'mse'; Metrics = 'mae'
Support vector machines (SVM)	Kernels C value	Kernel = 'poly'; Degree = 2 C = 100; Epsilon = 0.1
K-nearest neighbors (k-NN)	Number of neighbors	n_Neighbors = 3
Decision tree (DT)	Max depth Random state	Criterion = 'Gini'; Max_depth = 5 Ccp_alpha = 0.0; Min_samples_leaf = 1 Random_state = 100
Random forest (RF)	Number of estimators Max depth	Criterion = 'entropy'; N_estimators = 10; Max_depth = 5; Min_samples_leaf = 1; Min_sanmples_split = 2

2.4. Model Performance Evaluations

In order to analyze the performance of the predictive models, the confusion matrix and errors table concluded that accuracy evaluation indexes (e.g., accuracy, precision, recall, and f1-score), mean squared error (MSE), mean absolute error (MAE), and root mean square error (RMSE) were used. A confusion matrix is a specific table layout that allows the visualization of the performance of a machine learning algorithm, commonly used in supervised learning (in unsupervised learning, it is called a matching matrix). Each row of the matrix represents the instances in an actual class, while each column represents the instances in a predicted class [32]. Thus, in predictive analytics, a confusion matrix can be defined as a table with two rows and two columns that reports the number of true positives, false negatives, false positives, and true negatives. This allows more detailed analysis than simply observing the proportion of correct classifications (accuracy). Accuracy will yield misleading results if the data set is unbalanced, that is, when the numbers of observations in different classes vary greatly [33]. However, the performance matrix, which includes the parameters for accuracy, precision, recall, and f1-score, is a specific table that illustrates the performance of a prediction algorithm based on its predicted values (also known as evaluation indexes). True positives (TPs), true negatives (TNs), false positives (FPs), and false negatives (FNs) are used for classification tasks to compare the results of the classifier under consideration with reliable outside assessments [32]. So, each confusion matrix provides evaluation indexes that are used for the analysis of the machine learning classifiers' capability and performances. Precision (also called positive predictive value) is the fraction of relevant instances among the retrieved instances, while recall is the fraction of relevant instances that were retrieved, which is calculated as [33]:

$$\text{Precision} = \frac{\text{TP}}{\text{TP} + \text{FP}} \tag{1}$$

$$\text{Recall} = \frac{\text{TP}}{\text{TP} + \text{FN}} \tag{2}$$

The f1-score, which is the harmonic mean of precision and recall, provides approximately the average of the two values when they are close, and is more generally the harmonic mean [33]:

$$\text{f1-score} = 2 \cdot \frac{\text{Precision} \cdot \text{Recall}}{\text{Precision} + \text{Recall}} \tag{3}$$

The accuracy is the probability that a test will correctly classify a person; it is calculated by dividing the total number of true positives and true negatives by the total number of people who were tested [33]:

$$\text{Accuracy} = \frac{\text{TP} + \text{TN}}{\text{TP} + \text{TN} + \text{FP} + \text{FN}} \tag{4}$$

The errors table, including MAE, MSE, and RMSE, are the other performance investigators in the predictive models. These relationships are frequently used to quantify the discrepancies between values that are predicted by models and those that are determined by tests [32]:

$$\text{MAE} = \frac{\sum_{t=1}^{n} |y_i - x_i|}{n} \tag{5}$$

$$\text{MSE} = \frac{1}{n} \sum_{i=1}^{n} (y_i - x_i)^2 \tag{6}$$

$$\text{RMSE} = \sqrt{\frac{\sum_{t=1}^{n} (y_i - x_i)^2}{n}} \tag{7}$$

where the measured value is x_i and the predicted value is y_i. The application of these indicators shows that the algorithms perform better when there is less computational error. The performance of the predictive model was assessed in this study using a confusion matrix and errors table.

3. Results and Discussion

After creating the testing and training data sets from the primary database at random, the models were trained and tested to predict the target (FS) values. The FS was predicted based on the FS_{min} of the specific factors presented in Table 1 were estimated from the field via labeled data (supervised). The rotation estimation (cross-validation) procedure was used to predict how well a predictive model would perform in practice. The rotation estimation is a resampling method that tests and trains a model on different iterations using different portions of the data [33]. The equal-fold cross-validation method was used in this study to create equal-sized subsets (1:6 | 1 for reserved and 6 for training). Figures 3 and 4 show the prediction results for the various classifiers in the training and testing sets. According to the results presented in these figures, the predicted values of the FS in the MLP training set were close to the actual (estimated) values. The K-NN and DT correctly predicted the FS, but the SVM and RF differed from the actual values in the other predictive models. Meanwhile, the predictive models' predicted the FS values from the testing set follow the same pattern as the training set. During the training stage, the predictive models were trained regarding the stability evaluation based on the labeled geotechnical properties and the estimated FS (supervised) and then tested in a testing set that was responsible for the performance and precision of the applied models. The prediction and capability of the forecasting for both the training and testing sets are shown in Figures 4 and 5. In these figures, the prediction target is the FS value.

The confusion matrix and errors table concluded the evaluations of the predictive models. The MAE, MSE, and RMSE indexes were calculated for the different classifiers, and the results are shown in Tables 3 and 4. According to the results of the performance analysis, a higher value for the accuracy and precision parameters indicates that the models performed better. In this regard, the MLP model achieved the highest accuracy (0.938) and precision values (0.90). The MLP was followed by the k-NN and DT, which had estimated 0.849 accuracy and 0.808 accuracy values, respectively. With a 0.700 accuracy value, the RF had the lowest rate of prediction of the FS in the database. The MLP model, on the other hand, had the lowest errors among all classifiers, according to the results of the errors table, with an MAE = 0.103367, MSE = 0.102566, and RMSE = 0.098470. Other classifiers reached the same conclusion as the SVM: MAE = 0.145631, MSE = 0.130764, and RMSE = 0.128836. MAE = 0.125682, MSE = 0.123009, and RMSE = 0.120957 for k-NN. DT = 0.125369, MSE = 0.121942, and RMSE = 0.120454. RF: MAE = 0.138980, MSE = 0.135124, and RMSE = 0.126821.

Regarding the achieved results, the MLP model had the highest accuracy. By reviewing the literature in which different researchers used similar machine learning methods, it can be stated that the MLP is a superior classifier to the SVM, k-NN, DT, and RF. Table 5 provides a comparison of the different machine learning applications from selected scientific papers with the results of this study. According to this table, the present article provides the highest accuracy among the different predictive models. The selected papers were chosen based on the FS calculations from recent developments of the relevant predictive models.

Table 3. The performance matrix for further predictive models.

Classifier	Parameter	Assessment Score			Accuracy
		Precision	Recall	F1-Score	
MLP	Stable	0.90	0.88	0.90	0.938
	Unstable	0.90	0.90	0.89	
SVM	Stable	0.73	0.73	0.74	0.756
	Unstable	0.77	0.75	0.75	
k-NN	Stable	0.85	0.84	0.84	0.849
	Unstable	0.85	0.80	0.85	
DT	Stable	0.83	0.85	0.83	0.808
	Unstable	0.80	0.80	0.80	
RF	Stable	0.70	0.67	0.70	0.700
	Unstable	0.65	0.70	0.65	

Table 4. The errors estimated for different predictive models.

Classifier	MAE	MSE	RMSE
MLP	0.103367	0.102566	0.098470
SVM	0.145631	0.130764	0.128836
k-NN	0.125682	0.123009	0.120957
DT	0.125369	0.121942	0.120454
RF	0.138980	0.135124	0.126821

Table 5. Literature comparison for different predictive models based on FS calculations.

Aim	Applied Models	Target Model	Accuracy	Precision	Reference
FS calculation	LR, DT, RF, GBM, SVM, MLP	MLP	0.84	-	[17]
	RF, DT, SVM, k-NN, GBDT, AdaBoost, Bagging, MLP	MLP	0.88	-	[18]
	AdaBoost, GBM, Bagging, ET, RF, MLP	MLP	0.84	-	[34]
	MLP, GPR, MLR, SVM, SLR	SVM	-	-	[35]
	MLP, RBFR, MLR, SVM, k-NN, RF, RT	MLP	0.50	-	[22]
	BR, LR, ENR, ABR, SVM, GBR, ETR, DTR, KNR, Bagging	SVM	0.86	-	[36]
	MLP, SVM, k-NN, DT, RF	MLP	0.938	0.90	This study

Note(s): logistic regression (LR), gradient boosting machine (GBN), guided clustering algorithm (Bagging), gradient boosting decision tree (GBDT), extra trees (ET), Gaussian process regression (GPR), multiple linear regression (MLR), simple linear regression (SLR), radial basis function regression (RBFR), and random tree (RT).

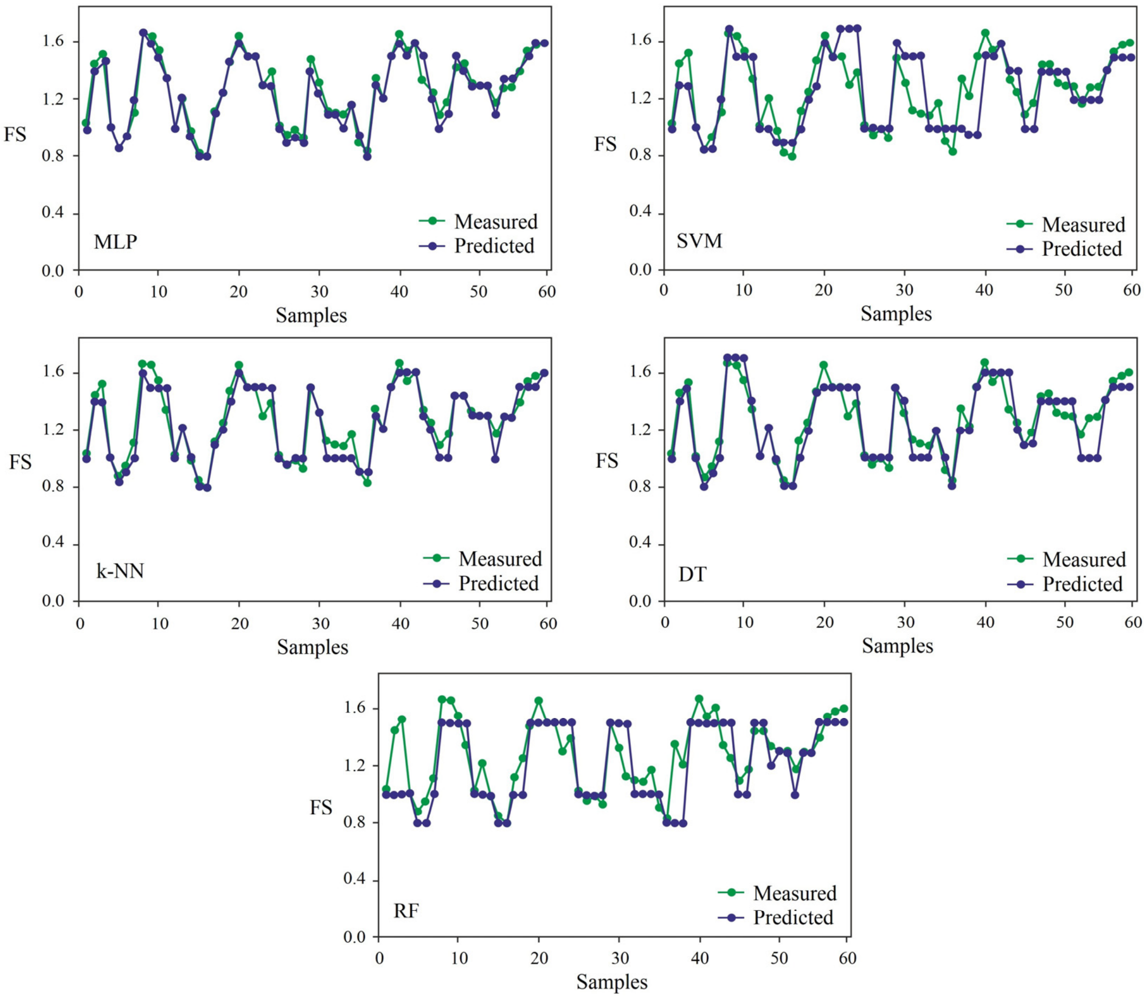

Figure 3. Results of the FS prediction in the training set by machine learning-based models.

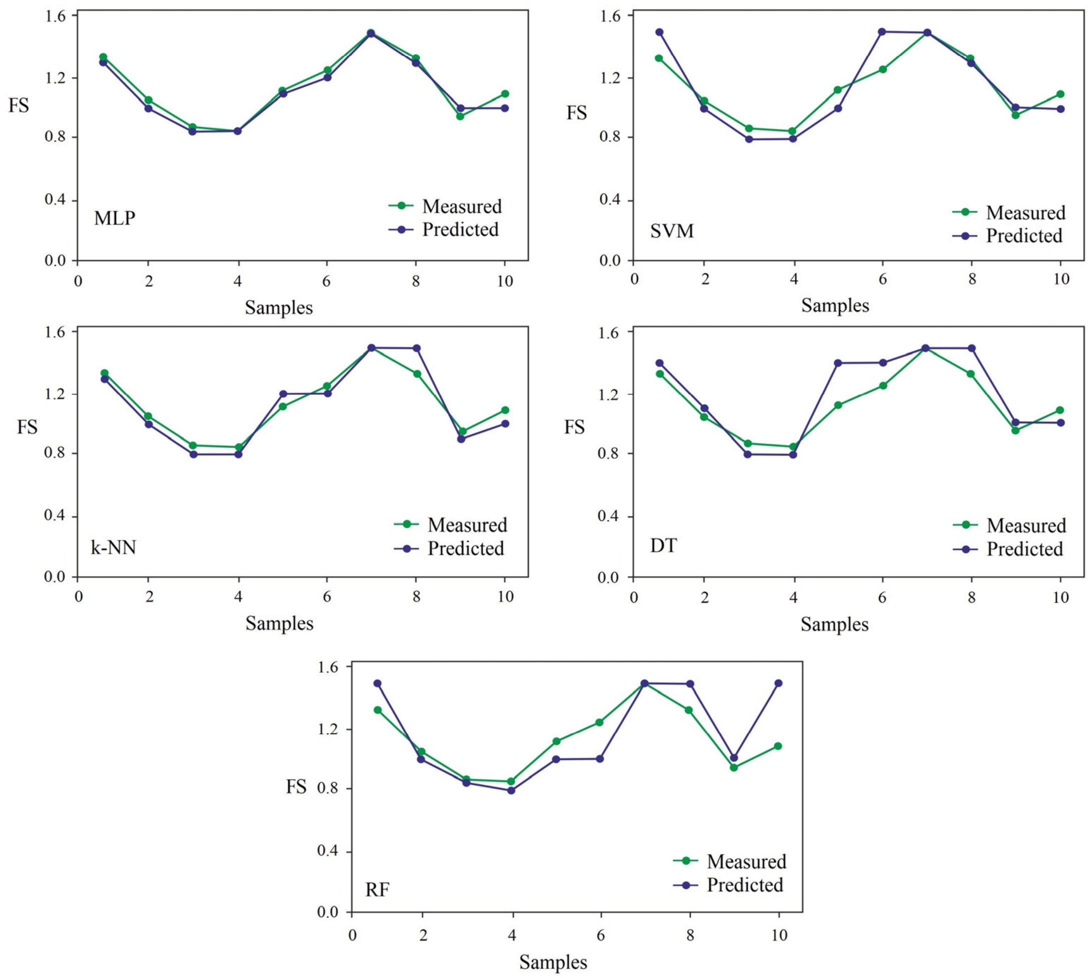

Figure 4. Results of the FS prediction in the testing set by machine learning-based models.

To validate and implement the predictive models, an example case was chosen from the primary data set. The slope was near the main Assalouyeh–Kangan highway in the northern part of the South Pars region. The chosen slope was at 27.542912, 52.58644, close to the phase 6 flare site. The studied slope, presented in Figure 5, is geologically composed of quaternary alluvium, with marls from the Aghajari formation. A field survey was conducted, and samples were collected to investigate the slope's stability condition. Table 6 provides the applied data for the studied slope regarding stability analysis. This information was recorded by field and laboratory works. During the field recording, topographical properties, such as slope height, slope angle, and slope geometry, as well as the geotechnical properties of the materials from the samples, were estimated. The predictive models and the well-known commercial SLIDE program [37] used the measured features for the stability analysis. Rocscience Inc. developed SLIDE, a 2D slope stability program for evaluating the factor of safety, or probability of failure, of circular and noncircular failure surfaces in soil or rock slopes. SLIDE evaluates the slope stability based on limit equilibrium procedures (vertical slice limit equilibrium methods) to obtain the FS for circular or noncircular failure surfaces. The program's design is user-friendly and operates automatically. The modeling was implemented in different steps concluding geometrical modeling, boundary conditions, behavioral criteria, materials, and mechanical modeling. In the geometrical modeling stage, each slope is modeled based on the topographical conditions, domain height, angle of the slope's surface, and other geometric index characteristics. The boundary conditions are implemented by the 'External Boundary', which is a closed polyline encompassing the soil region you wish to analyze. In addition, it can be entered graphically in SLIDE by simply clicking the left mouse button at the desired coordinates. The present work used graphical coordinates. The Mohr–Coulomb failure criterion was selected for the stability analysis in the behavioral criteria selection. In the materials assignment stage, the geotechnical properties of the soils used are presented in Table 1. The data in this table were provided based on the performance of various geotechnical tests. After the preparation of the model, the model was analyzed regarding stability in the mechanical modeling. In this stage, the slope was examined using the Bishop and Janbu limit equilibrium analysis methods (the program's default). The model can be changed by other limit equilibrium in the 'Analysis Methods dialog' section. The present study used a default procedure. The SLIDE program's stability analysis results are shown in Figure 6. Table 7 contains information regarding the FS. Predictive model and SLIDE program results. With their justification method, predictive models, particularly MLP, provide close results to FS value, according to this table.

Table 6. The geotechnical information used for the example stability analysis.

Parameter	Unit	Value
Specific gravity (G_s)	-	2.63
γ_d	kN/m^3	20.00
Slope height (H)	m	14.5
Slope angle (β)	Degree	65
Cohesion (c)	kPa	125
Friction (φ)	Degree	35

Table 7. FS evaluation by different models for the selected slope.

No.	Analysis Method	Estimated FS
1	MLP	1.18
2	SVM	1.1
3	DT	1.1
4	RF	1.4
5	SLIDE	1.21

Figure 5. A view of the selected slope in the South Pars region.

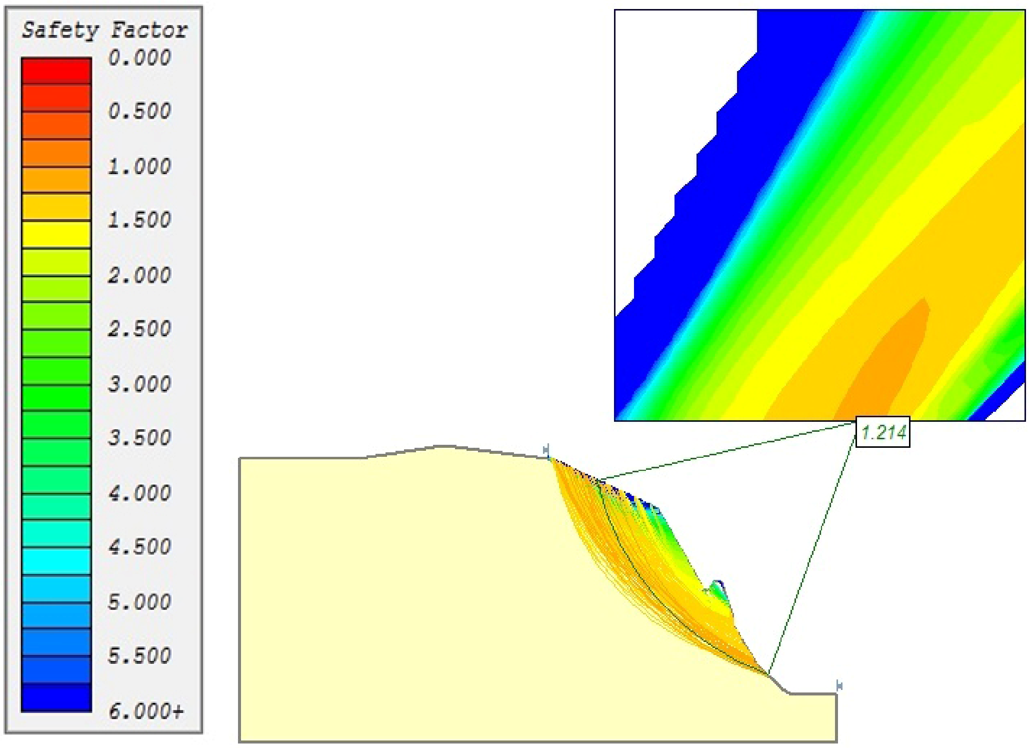

Figure 6. Stability analysis of the selected slope by SLIDE.

4. Conclusions

This study attempted to provide slope stability by using various machine learning-based techniques, including multilayer perceptron (MLP), support vector machines (SVM), K-nearest neighbors (k-NN), decision tree (DT), and random forest (RF), and aimed to establish a highly accurate predictive model for predicting the factor of safety (FS). The aim of the application of several machine learning methods was to investigate a highly accurate predictive model to predict/estimate the FS. For the primary analysis database, 70 recorded slope cases from South Pars were used. The FS was picked as output, and the index geotechnical properties of the slope (c, φ, H, β, and γ_d) were picked as input data. The implementation of the models was carried out in the Python high-level programming language. The results were reported for each stage and utilized to calculate the predictive models' performances. A confusion matrix and errors table were used for the model performance evaluations. According to the results of the modeling, they indicated that the MLP model reached the highest values of accuracy (0.938) and precision (0.90). The k-NN and DT, with 0.849 and 0.808 accuracy, respectively, were followed by the MLP. The RF obtained the lowest rate of prediction for the FS in the database, with 0.700. On the other hand, according to the results of the errors table, the MLP model, with MAE = 0.103367, MSE = 0.102566, and RMSE = 0.098470, reached the lowest errors among all of the classifiers. Regarding the mentioned results, the MLP showed a difference with other classifiers, but it had a slight discrepancy with the k-NN. Therefore, it can be stated that after MLP, k-NN can provide reliably predicted FS values.

Author Contributions: Y.A.N. and J.C. (Jin Chengyong): writing—original draft preparation, validation, methodology, investigation, and resources; T.P., J.C. (Junde Chen) and A.C.: visualization and methodology; M.A. and R.D.: supervision, formal analysis, conceptualization, and writing—review and editing. All authors have read and agreed to the published version of the manuscript.

Funding: This research received no external funding.

Informed Consent Statement: Not applicable.

Data Availability Statement: Not applicable.

Acknowledgments: The authors wish to thank the Department of Civil Engineering, University of Tabriz, for providing permission to conduct the geotechnical investigations. In addition, the authors would like to thank the anonymous reviewers for providing invaluable review comments and recommendations for improving the scientific level of the article.

Conflicts of Interest: The authors declare no conflict of interest.

Abbreviations

FS	Factor of safety	MLP	Multilayer perceptron
H	Slope height	SVM	Support vector machines
β	Slope angle	k-NN	k-nearest neighbors
γ_d	Dry density	DT	Decision tree
c	Cohesion	RF	Random forest
ϕ	Internal friction angle	TP	True positive
S_u	Total cohesion	TN	True negative
C_u	Undrained cohesion	FP	False positive
Gs	Specific gravity	FN	False negative
R	Forces resultant vector	MSE	Mean squared error
W	Movable mass weight	MAE	Mean absolute error
c'	Effective cohesion	RMSE	Root mean square error
ϕ'	Effective friction angle		

References

1. Azarafza, M.; Akgün, H.; Ghazifard, A.; Asghari-Kaljahi, E.; Rahnamarad, J.; Derakhshani, R. Discontinuous rock slope stability analysis by limit equilibrium approaches—A review. *Int. J. Digit. Earth* **2021**, *14*, 1918–1941. [CrossRef]
2. Azarafza, M.; Hajialilue Bonab, M.; Derakhshani, R. A novel empirical classification method for weak rock slope stability analysis. *Sci. Rep.* **2022**, *12*, 14744. [CrossRef]
3. Huang, Y.H. *Slope Stability Analysis by the Limit Equilibrium Method*; ASCE Publications: Reston, VA, USA, 2014.
4. Abramson, L.W.; Lee, T.S.; Sharma, S.; Boyce, G.M. *Slope Stability Concepts: Slope Stabilisation and Stabilisation Methods*, 2nd ed.; Wiley-Interscience: Millburn, NJ, USA, 2001.
5. Azarafza, M.; Nikoobakht, S.; Asghari-Kaljahi, E.; Moshrefy-Far, M.R. Stability analysis of jointed rock slopes using block theory (case study: Gas flare site in phase 7 of South Pars Gas Complex). In Proceedings of the 32th National & 1st International Geosciences Congress of Iran, Tehran, Iran, 3–4 February 2014.
6. Agam, M.W.; Hashim, M.H.M.; Murad, M.I.; Zabidi, H. Slope Sensitivity Analysis Using Spencer's Method in Comparison with General Limit Equilibrium Method. *Procedia Chem.* **2016**, *19*, 651–658. [CrossRef]
7. Alejano, L.; Ferrero, A.M.; Ramírez-Oyanguren, P.; Álvarez Fernández, M.I. Comparison of Limit-Equilibrium, Numerical and Physical Models of Wall Slope Stability. *Int. J. Rock Mech. Min. Sci.* **2011**, *48*, 16–26. [CrossRef]
8. Chakraborty, A.; Goswami, D. State of the art: Three dimensional (3D) slope-stability analysis. *Int. J. Geotech. Eng.* **2016**, *10*, 493–498. [CrossRef]
9. Bromhead, E. *The Stability of Slopes*; Spon Press: New York, NY, USA, 1992.
10. Mafi, R.; Javankhoshdel, S.; Cami, B.; Jamshidi Chenari, R.; Gandomi, A.H. Surface altering optimisation in slope stability analysis with non-circular failure for random limit equilibrium method. *Georisk Ass. Manag. Risk Eng. Sys. Geohaz.* **2021**, *15*, 260–286. [CrossRef]
11. Chen, Z.; Mi, H.; Zhang, F.; Wang, F. A Simplified Method for 3D Slope Stability Analysis. *Can. Geotech. J.* **2003**, *40*, 675–683. [CrossRef]
12. Correia, R.M. A limit equilibrium method of slope stability analysis. In Proceedings of the 5th International Symposium on Landslides, Lausanne, Switzerland, 10–15 July 1988.
13. Deng, D. Limit Equilibrium Solution for the Rock Slope Stability under the Coupling Effect of the Shear Dilatancy and Strain Softening. *Int. J. Rock Mech. Min. Sci.* **2020**, *134*, 104421. [CrossRef]
14. Biniyaz, A.; Azmoon, B.; Liu, Z. Coupled transient saturated–unsaturated seepage and limit equilibrium analysis for slopes: Influence of rapid water level changes. *Acta Geotech.* **2022**, *17*, 2139–2156. [CrossRef]
15. Zhou, J.; Li, E.; Yang, S.; Wang, M.; Shi, X.; Yao, S.; Mitri, H.S. Slope Stability Prediction for Circular Mode Failure Using Gradient Boosting Machine Approach Based on an Updated Database of Case Histories. *Saf. Sci.* **2019**, *118*, 505–518. [CrossRef]
16. Wei, W.; Li, X.; Liu, J.; Zhou, Y.; Li, L.; Zhou, J. Performance Evaluation of HybridWoa-Svr and Hho-Svr Models with Various Kernels to Predict Factor of Safety for Circular Failure Slope. *Appl. Sci.* **2021**, *11*, 1922. [CrossRef]
17. Qi, C.; Tang, X. Slope stability prediction using integrated metaheuristic and machine learning approaches: A comparative study. *Comput. Ind. Eng.* **2018**, *118*, 112–122. [CrossRef]

18. Bai, G.; Hou, Y.; Wan, B.; An, N.; Yan, Y.; Tang, Z.; Yan, M.; Zhang, Y.; Sun, D. Performance Evaluation and Engineering Verification of Machine Learning Based Prediction Models for Slope Stability. *Appl. Sci.* **2022**, *12*, 7890. [CrossRef]
19. Zhang, Y.; Dai, M.; Ju, Z. Preliminary discussion regarding SVM kernel function selection in the twofold rock slope prediction model. *J. Comput. Civ. Eng.* **2015**, *30*, 04015031. [CrossRef]
20. Chakraborty, A.; Goswami, D. Prediction of slope stability using multiple linear regression (MLR) and artificial neural network (ANN). *Arab. J. Geosci.* **2017**, *10*, 11. [CrossRef]
21. Jagan, J.; Meghana, G.; Samui, P. Determination of stability number of layered slope using ANFIS, GPR, RVM and ELM. *Int. J. Comput. Res.* **2016**, *23*, 371.
22. Bui, D.T.; Moayedi, H.; Gör, M.; Jaafari, A.; Foong, L.K. Predicting slope stability failure through machine learning paradigms. *ISPRS Int. J. Geo-Inform.* **2019**, *8*, 395. [CrossRef]
23. Bardhan, A.; Samui, P. Probabilistic slope stability analysis of Heavy-haul freight corridor using a hybrid machine learning paradigm. *Transport. Geotech.* **2022**, *37*, 100815. [CrossRef]
24. Karir, D.; Ray, A.; Bharati, A.K.; Chaturvedi, U.; Rai, R.; Khandelwal, M. Stability prediction of a natural and man-made slope using various machine learning algorithms. *Transport. Geotech.* **2022**, *34*, 100745. [CrossRef]
25. Omar, M.; Che Mamat, R.; Abdul Rasam, A.R.; Ramli, A.; Samad, A. Artificial intelligence application for predicting slope stability on soft ground: A comparative study. *Int. J. Adv. Technol. Eng. Explor.* **2021**, *8*, 362–370. [CrossRef]
26. *ASTM D2166*; Standard Test Method for Unconfined Compressive Strength of Cohesive Soil. ASTM International: West Conshohocken, PA, USA, 2006.
27. *ASTM D3080*; Standard Test Method for Direct Shear Test of Soils under Consolidated Drained Conditions. ASTM International: West Conshohocken, PA, USA, 2004.
28. Zhou, J.; Qin, C. A Novel Procedure for 3D Slope Stability Analysis: Lower Bound Limit Analysis Coupled with Block Element Method. *Bull. Eng. Geol. Environ.* **2020**, *79*, 1815–1829. [CrossRef]
29. Azarafza, M.; Asghari-Kaljahi, E.; Akgün, H. Assessment of Discontinuous Rock Slope Stability with Block Theory and Numerical Modeling: A Case Study for the South Pars Gas Complex, Assalouyeh, Iran. *Environ. Earth Sci.* **2017**, *76*, 397. [CrossRef]
30. Zhu, D.Y.; Lee, C.F.; Jiang, H.D. Generalised Framework of Limit Equilibrium Methods for Slope Stability Analysis. *Geotechnique* **2003**, *53*, 377–395. [CrossRef]
31. Lam, L.; Fredlund, L. A General Limit Equilibrium Model for Three-Dimensional Slope Stability Analysis. *Can. Geotech. J.* **1993**, *30*, 905–919. [CrossRef]
32. Müller, A.C.; Guido, S. *Introduction to Machine Learning with Python: A Guide for Data Scientists*; O'Reilly Media: Sebastopol, CA, USA, 2016.
33. Aggarwal, C.C. *Neural Networks and Deep Learning: A Textbook*; Springer: Berlin/Heidelberg, Germany, 2018.
34. Lin, S.; Zheng, H.; Han, B.; Li, Y.; Han, C.; Li, W. Comparative performance of eight ensemble learning approaches for the development of models of slope stability prediction. *Acta Geotech.* **2022**, *17*, 1477–1502. [CrossRef]
35. Moayedi, H.; Bui, D.T.; Kalantar, B.; Kok Foong, L. Machine-learning-based classification approaches toward recognizing slope stability failure. *Appl. Sci.* **2019**, *9*, 4638. [CrossRef]
36. Lin, S.; Zheng, H.; Han, C.; Han, B.; Li, W. Evaluation and prediction of slope stability using machine learning approaches. *Front. Struct. Civ. Eng.* **2021**, *15*, 821–833. [CrossRef]
37. Rocscience Inc. Slide Geotechnical Software. Available online: https://www.rocscience.com/software/slide2 (accessed on 1 August 2022).